Supplement of Geosci. Model Dev., 16, 1163–1178, 2023
https://doi.org/10.5194/gmd-16-1163-2023-supplement

Geoscientific Model Development
Open Access

Supplement of

Multidecadal and climatological surface current simulations for the southwestern Indian Ocean at $1/50^{\circ}$ resolution

Noam S. Vogt-Vincent and Helen L. Johnson

Correspondence to: Helen L. Johnson (helen.johnson@earth.ox.ac.uk)

Supplementary Tables

Site	Longitude	Latitude	Tide	WINDS (cm)	WINDS - TPXO9 (cm)
Coastal sites					
Réunion	55.2	-20.9	M2	17.2	2.6
France			S2	6.7	-1.0
			N2	4.5	0.6
			K1	5.1	-0.2
			O1	2.9	0.1
Mayotte	45.3	-13.0	M2	105.4	-3.0
France			S2	55.9	6.1
			N2	17.6	-1.4
			K1	13.7	-1.1
			O1	7.9	0.1
Glorioso Islands	47.3	-11.5	M2	91.3	-2.3
France			S2	47.3	5.0
			N2	16.8	-0.2
			K1	14.6	-1.4
			O1	8.1	-0.1
Mauritius	57.8	-20.4	M2	25.5	1.8
Mauritius			S2	14.2	2.1
			N2	5.2	0.4
			K1	6.0	-0.8
			O1	2.5	-0.2
St. Brandon	59.6	-16.6	M2	23.6	2.7
Mauritius			S2	13.6	5.1
			N2	5.7	0.5
			K1	6.5	-1.8
			O1	3.6	-0.8
Rodrigues	63.4	-19.6	M2	41.3	1.4
Mauritius			S2	22.8	3.3
			N2	8.1	0.9
			K1	5.9	-1.5
			O1	3.3	0.2
Vingt Cinq	56.6	-10.4	M2	30.5	0.5
Mauritius			S2	13.3	3.0
			N2	7.7	0.5
			K1	10.4	-1.9
			O1	6.4	-0.3
Diego Garcia	72.4	-7.4	M2	47.6	0.1
Chagos			S2	28.2	3.6
			N2	8.7	0.4
			K1	3.6	-1.7
			O1	3.3	-0.2
Grand Chagos Bnk	72.0	-6.2	M2	42.6	-0.2
Chagos			S2	25.7	2.9
			N2	7.9	0.3
			K1	6.0	-0.5
			O1	3.6	-0.1

Blenheim Reef	72.5	-5.2	M2	42.7	3.5
Chagos			S2	25.5	4.7
			N2	7.4	0.6
			K1	6.4	-0.2
			O1	3.9	0.2
Fuvahmulah Atoll	73.4	-0.4	M2	29.4	0.0
Maldives			S2	18.4	2.6
			N2	4.9	0.4
			K1	8.9	-0.5
			O1	3.9	-0.6
Coëtivy	56.3	-7.2	M2	35.2	-1.0
Seychelles			S2	16.4	3.0
			N2	8.8	1.0
			K1	16.3	0.6
			O1	7.8	-0.1
Platte	55.3	-5.9	M2	40.8	-1.6
Seychelles			S2	19.4	2.7
			N2	8.7	0.2
			K1	16.1	-1.4
			O1	9.0	0.4
Mahé	55.4	-4.7	M2	41.8	-2.5
Seychelles			S2	19.6	1.6
			N2	8.4	-0.5
			K1	18.6	-0.4
			O1	9.1	0.1
Bird Island	55.2	-3.7	M2	36.7	-1.8
Seychelles			S2	16.6	0.7
			N2	7.6	0.3
			K1	21.1	-0.7
			O1	10.2	0.3
D Arros	53.3	-5.5	M2	53.4	-0.9
Seychelles			S2	24.0	1.1
			N2	9.4	-0.9
			K1	18.0	-1.5
			O1	9.3	-0.1
Alphonse Island	52.7	-7.0	M2	55.6	1.4
Seychelles			S2	26.4	3.9
			N2	10.1	-0.4
			K1	16.6	-1.1
			O1	8.9	-1.1
Farquhar Atoll	51.0	-10.2	M2	53.7	-5.6
Seychelles			S2	25.7	1.8
			N2	10.5	-1.1
			K1	13.1	-1.3
			O1	7.5	0.0
Aldabra Atoll	46.3	-9.3	M2	94.0	1.0
Seychelles			S2	47.4	5.6
			N2	16.5	-0.4

			K1	16.4	-1.3
			O1	8.9	0.0
Ngazidja	43.2	-11.6	M2	110.4	1.1
Comoros			S2	58.1	8.5
			N2	20.0	0.7
			K1	14.6	-1.1
			O1	8.4	0.1
Manakara	48.1	-22.2	M2	10.9	0.0
Madagascar			S2	6.1	0.3
			N2	2.8	-0.1
			K1	2.9	0.3
			O1	1.8	0.1
Fenerive	49.5	-17.3	M2	23.9	1.6
Madagascar			S2	10.3	2.4
			N2	5.7	0.0
			K1	3.7	0.3
			O1	3.5	0.2
Antongil Bay	49.9	-16.0	M2	29.4	-1.5
Madagascar			S2	13.6	3.7
			N2	7.1	-0.7
			K1	5.2	0.0
			O1	4.3	0.3
Helodr. Nar. Bay	47.5	-14.9	M2	114.5	-3.4
Madagascar			S2	61.4	6.4
			N2	19.9	-1.0
			K1	14.1	-0.7
			O1	7.1	-0.6
Hell-Ville	48.2	-13.6	M2	107.9	0.8
Madagascar			S2	56.8	7.7
			N2	19.5	-0.5
			K1	14.3	-1.2
			O1	7.9	-0.1
Cape Amber	49.2	-11.9	M2	75.6	-3.4
Madagascar			S2	36.8	2.6
			N2	14.6	0.0
			K1	13.8	-1.2
			O1	7.2	-0.5
Ankerefo	44.4	-16.2	M2	122.6	-9.0
Madagascar			S2	66.7	4.8
			N2	21.3	-1.0
			K1	11.7	-1.1
			O1	6.8	0.4
Belo Tsiribihina	44.4	-19.5	M2	113.8	-2.5
Madagascar			S2	65.9	7.7
			N2	19.0	-0.1
			K1	6.1	-0.3
			O1	4.3	0.0
Morombe	43.3	-21.8	M2	98.1	0.9
Madagascar			S2	57.3	8.2

			N2	16.2	0.5
			K1	5.0	-0.1
			O1	3.1	-0.1
Beira	34.9	-20.0	M2	129.1	-15.5
Mozambique			S2	76.1	4.5
			N2	20.8	-3.9
			K1	1.4	0.7
			O1	4.0	-0.1
Quelimane	37.1	-18.0	M2	112.6	0.4
Mozambique			S2	64.3	4.6
			N2	18.5	-0.1
			K1	3.3	0.3
			O1	4.7	0.2
Nacala	40.9	-14.5	M2	111.8	-2.4
Mozambique			S2	60.6	7.3
			N2	19.3	-0.5
			K1	10.9	-0.9
			O1	7.3	0.2
South Quirimbas	40.6	-12.5	M2	113.2	-2.6
Mozambique			S2	59.0	5.7
			N2	19.6	-0.7
			K1	13.2	-1.1
			O1	7.8	-0.1
North Quirimbas	40.6	-11.0	M2	109.9	-7.1
Mozambique			S2	56.9	3.8
			N2	18.9	-1.4
			K1	15.1	-1.0
			O1	8.6	0.2
Lindi	39.9	-9.9	M2	107.7	-1.0
Tanzania			S2	55.5	7.1
			N2	18.4	-0.8
			K1	16.7	-0.5
			O1	8.8	0.1
Mafia Island	39.7	-7.8	M2	111.4	-11.5
Tanzania			S2	57.0	1.5
			N2	20.1	-1.8
			K1	18.1	-1.2
			O1	9.2	-0.4
Zanzibar Channel	39.0	-6.3	M2	116.5	-11.0
Tanzania			S2	59.5	1.5
			N2	21.0	-2.0
			K1	18.6	-2.0
			O1	10.0	0.0
Pemba Island	39.9	-5.0	M2	100.9	-1.9
Tanzania			S2	52.2	6.8
			N2	18.8	0.5
			K1	19.9	-0.5
			O1	9.8	-0.1
Watamu	40.1	-3.5	M2	101.5	1.5
Kenya			S2	50.8	6.8
			N2	18.2	0.4

			K1	20.2	-0.6
			O1	10.2	0.2
Lamu *Kenya*	41.1	-2.3	M2	92.4	1.6
			S2	48.0	8.5
			N2	16.9	0.8
			K1	20.4	-0.6
			O1	10.8	1.1
Kismayo *Somalia*	42.6	-0.4	M2	85.0	-3.1
			S2	43.0	4.5
			N2	15.8	0.1
			K1	21.5	-1.7
			O1	11.4	0.5
Open ocean sites					
Moz. Channel N	42.5	-15.0	M2	114.5	-1.3
			S2	62.9	8.6
			N2	19.0	-0.9
			K1	11.1	-0.5
			O1	6.8	-0.1
Moz. Channel S	40.0	-20.0	M2	105.3	1.5
			S2	60.0	7.5
			N2	17.5	0.6
			K1	3.1	-0.1
			O1	3.4	-0.5
W Seychelles	45.0	-5.0	M2	90.3	0.5
			S2	45.5	5.6
			N2	16.4	0.2
			K1	19.8	-1.0
			O1	10.3	0.2
E Seychelles	65.0	-5.0	M2	21.8	0.1
			S2	13.0	1.2
			N2	4.9	0.5
			K1	13.4	-0.6
			O1	6.8	0.0
N Mascarene	55.0	-12.5	M2	29.4	-1.7
			S2	11.3	0.7
			N2	7.8	0.3
			K1	9.9	-0.6
			O1	6.4	0.4
Mascarene Plat.	61.4	-10.7	M2	26.0	0.0
			S2	14.4	1.8
			N2	6.4	0.5
			K1	9.6	-0.6
			O1	5.5	0.1
S Mascarene	52.5	-20.0	M2	16.4	1.4
			S2	7.1	0.5
			N2	4.1	-0.2
			K1	3.5	-0.4
			O1	2.6	-0.1

N Chagos	75.0	-2.5	M2	36.8	0.0
			S2	22.1	2.8
			N2	6.7	0.6
			K1	4.8	-0.0
			O1	3.1	0.2
S Chagos	70.0	-15.0	M2	52.6	-1.1
			S2	31.3	3.5
			N2	9.8	0.1
			K1	6.7	0.0
			O1	3.6	0.0

Table S1: *Amplitudes of the 5 largest tidal constituents at 50 coastal and open-ocean sites across the SWIO, extracted from WINDS (based on the first 55 days of WINDS-M_1994 with the free surface output at 2-hourly frequency) using t_tides, compared to predictions from TPXO9-atlas* (Egbert & Erofeeva, 2002)

Supplementary Figures

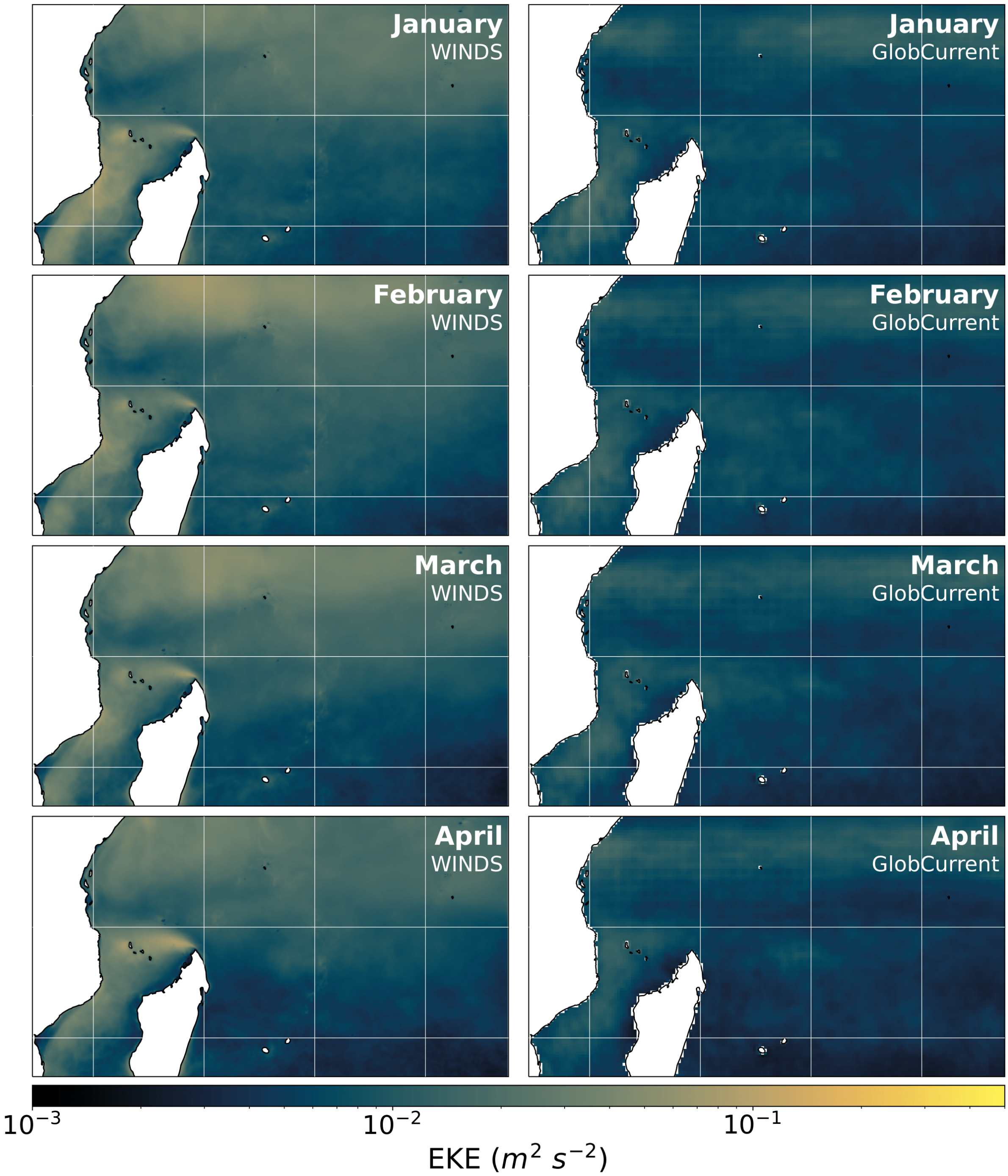

Figure S1: EKE for January-April in WINDS (left) and Copernicus GlobCurrent (right).

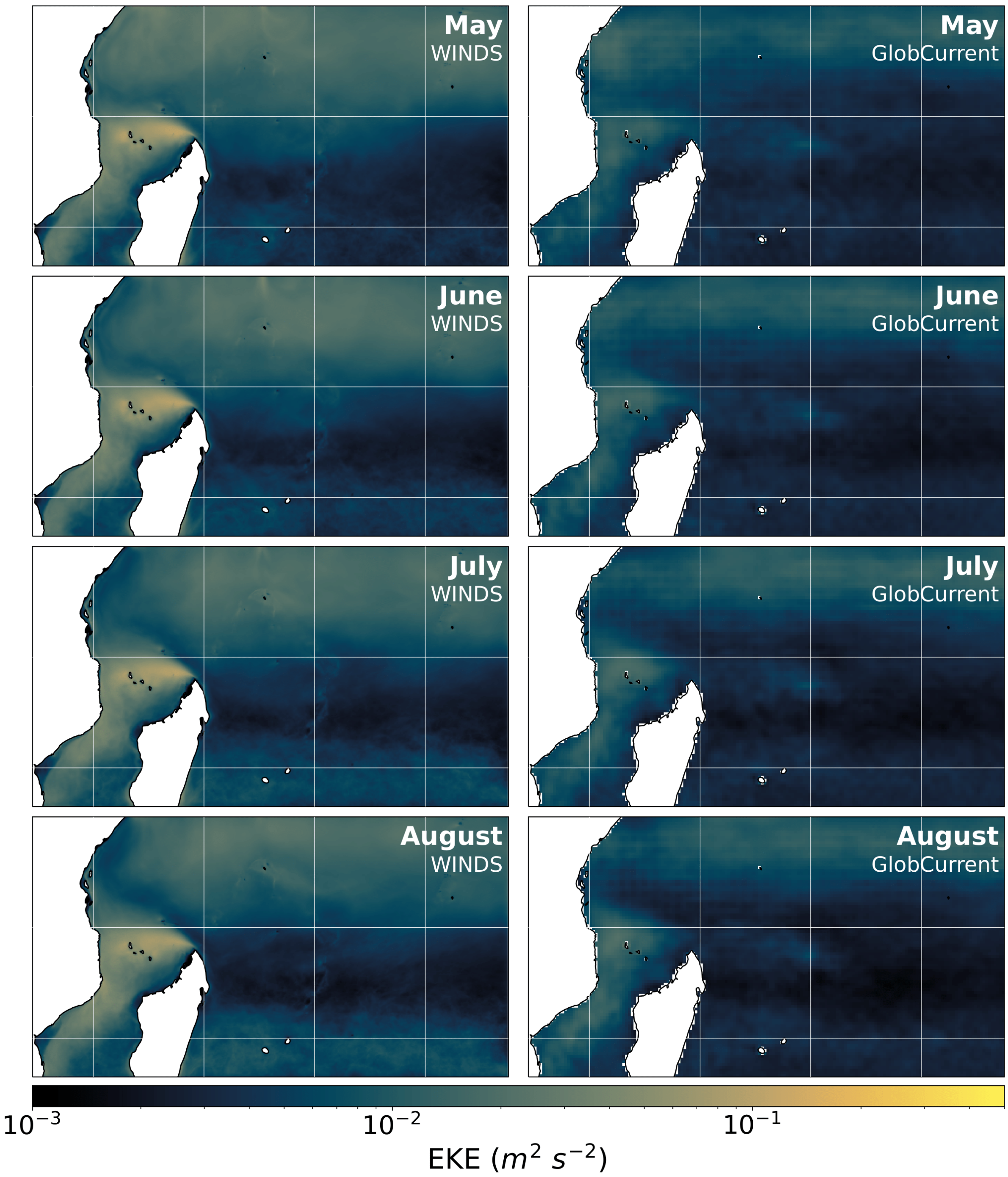

Figure S2: EKE for May-August in WINDS (left) and Copernicus GlobCurrent (right).

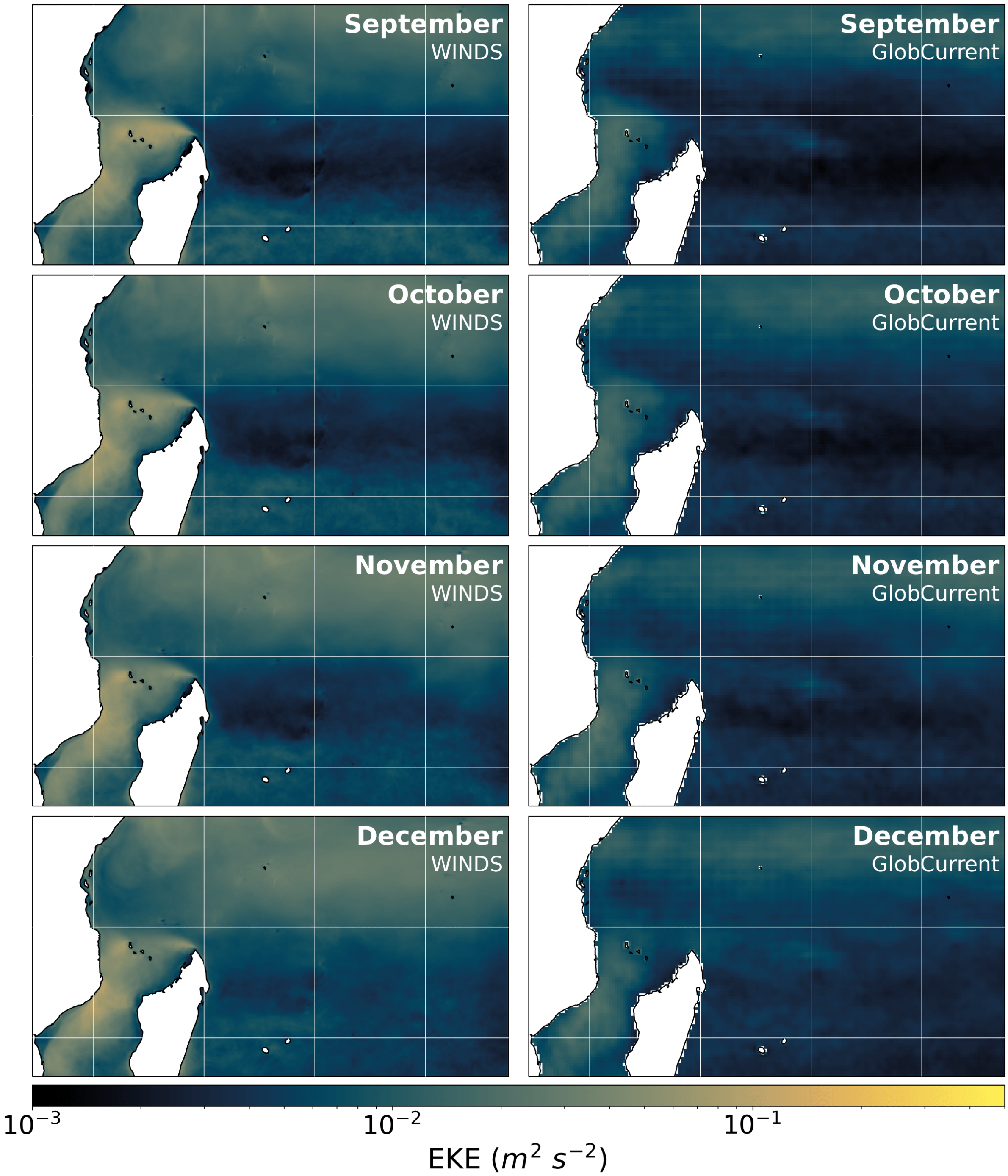

Figure S3: EKE for September-December in WINDS (left) and Copernicus GlobCurrent (right).

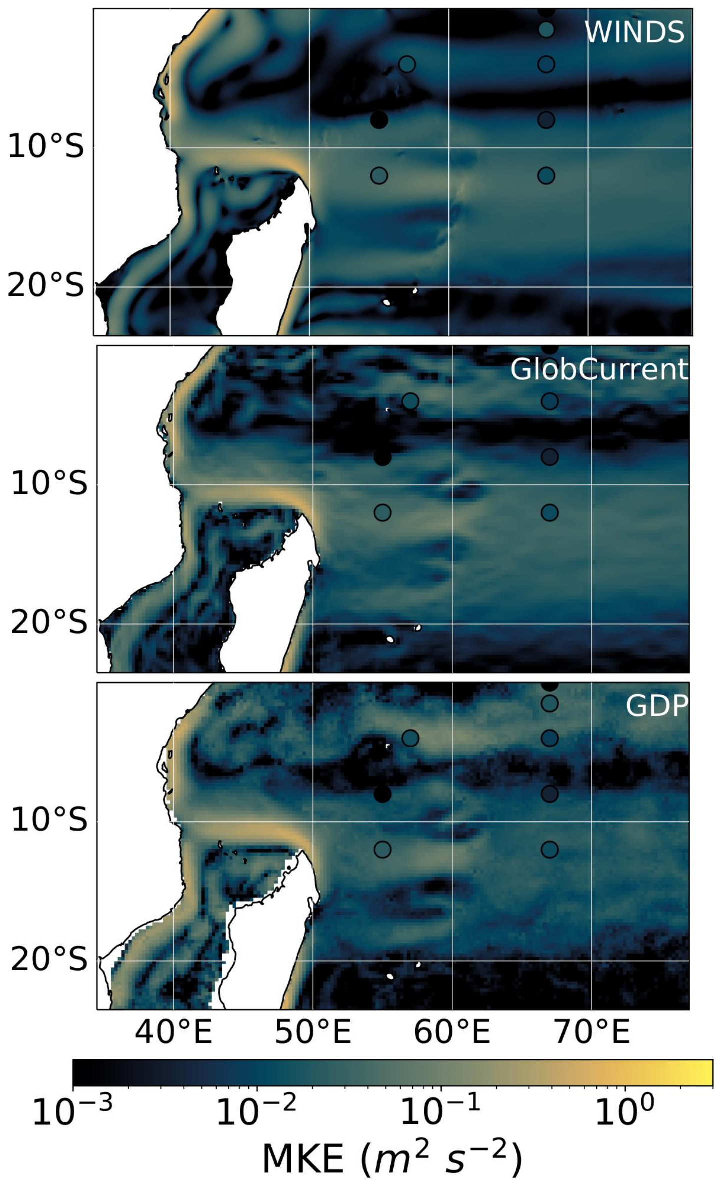

Figure S4: *Mean Kinetic Energy (MKE) computed from the time-mean velocity field, from WINDS (top), Copernicus GlobCurrent (centre), and surface velocities based on Global Drifter Program floats (bottom).*

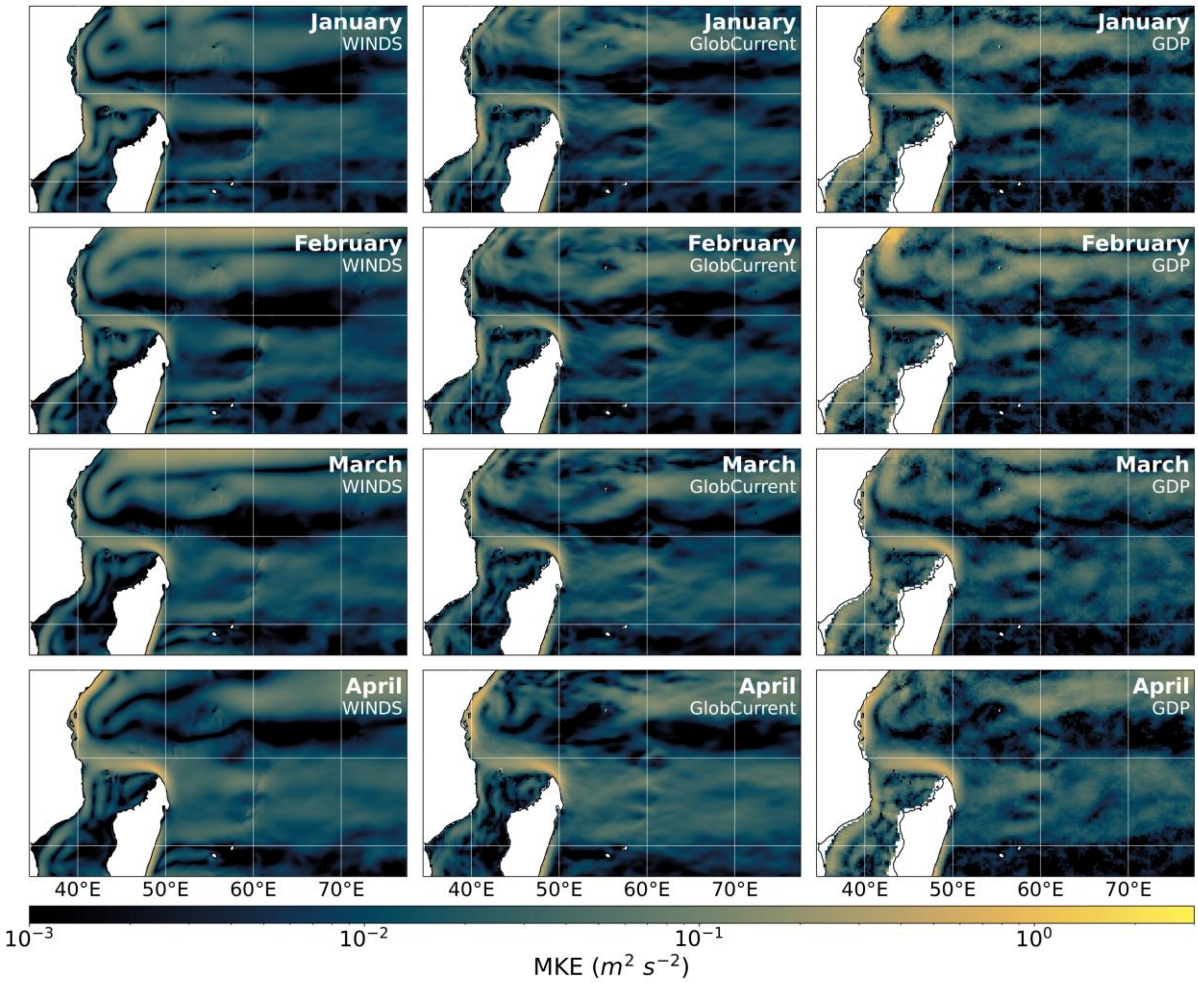

Figure S5: MKE for January-April from WINDS (left), Copernicus GlobCurrent (centre), and surface velocities from the Global Drifter Program (right).

:

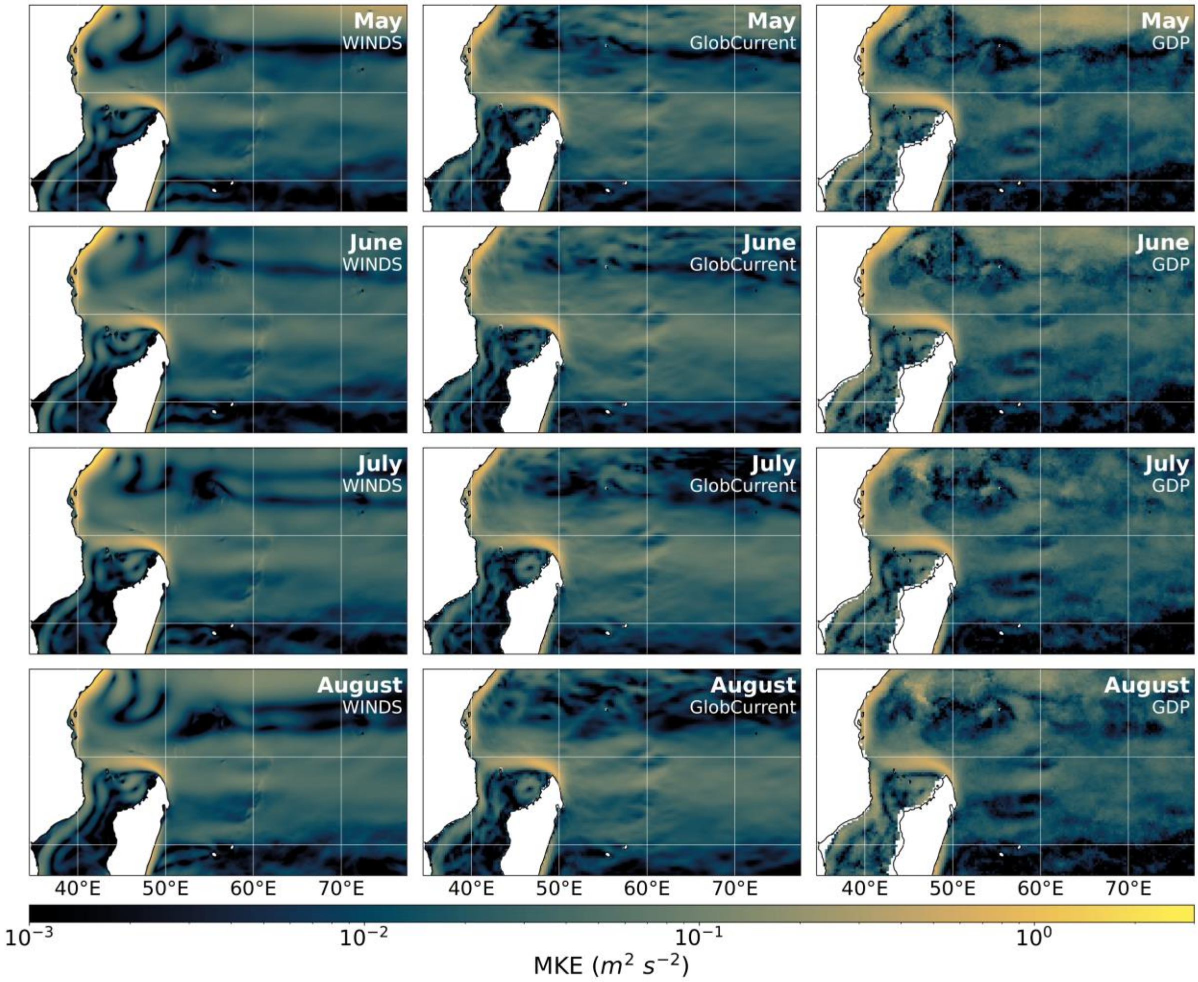

Figure S6: MKE for May-August from WINDS (left), Copernicus GlobCurrent (centre), and surface velocities from the Global Drifter Program (right).

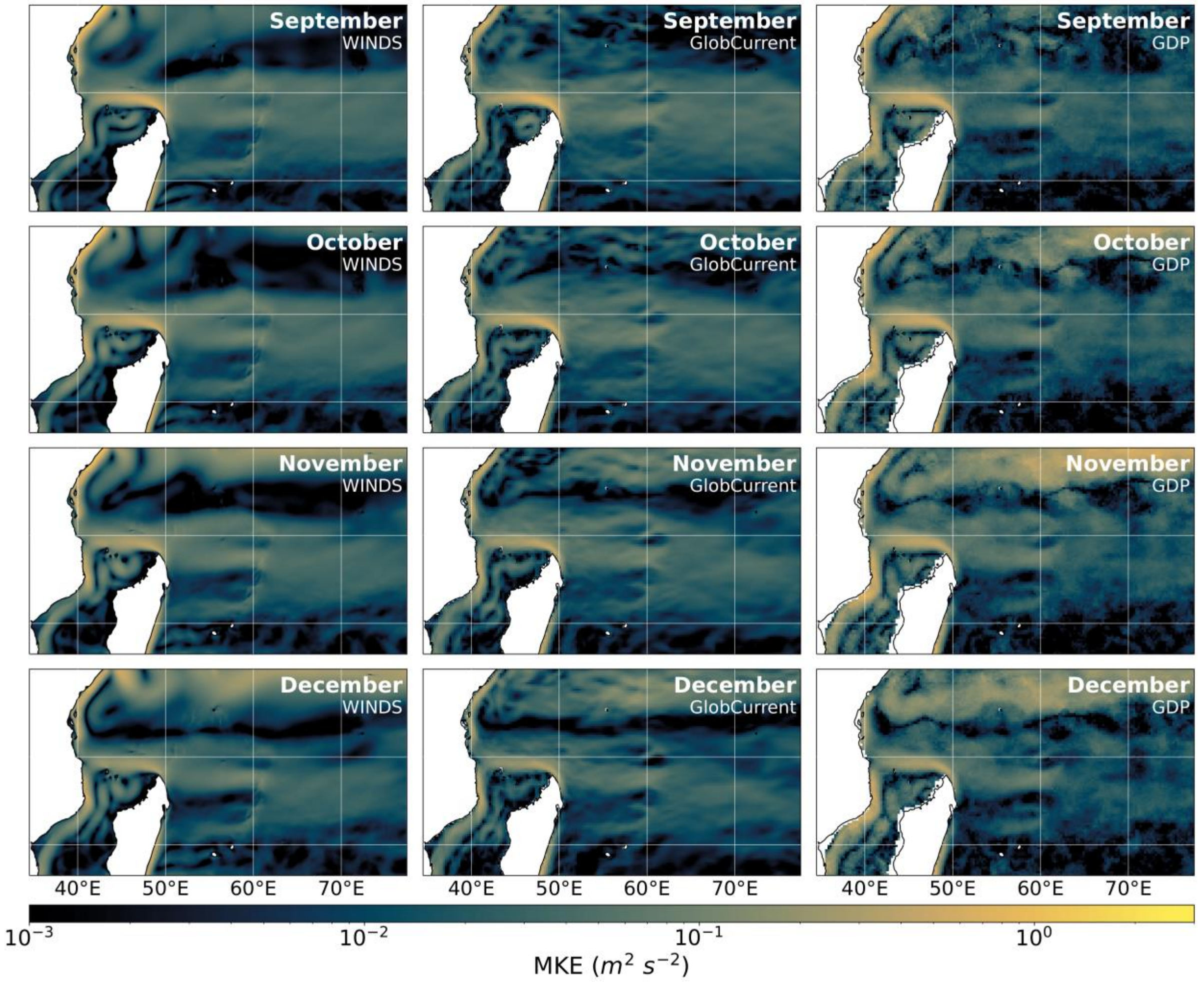

Figure S7: *MKE for September-December from WINDS (left), Copernicus GlobCurrent (centre), and surface velocities from the Global Drifter Program (right).*

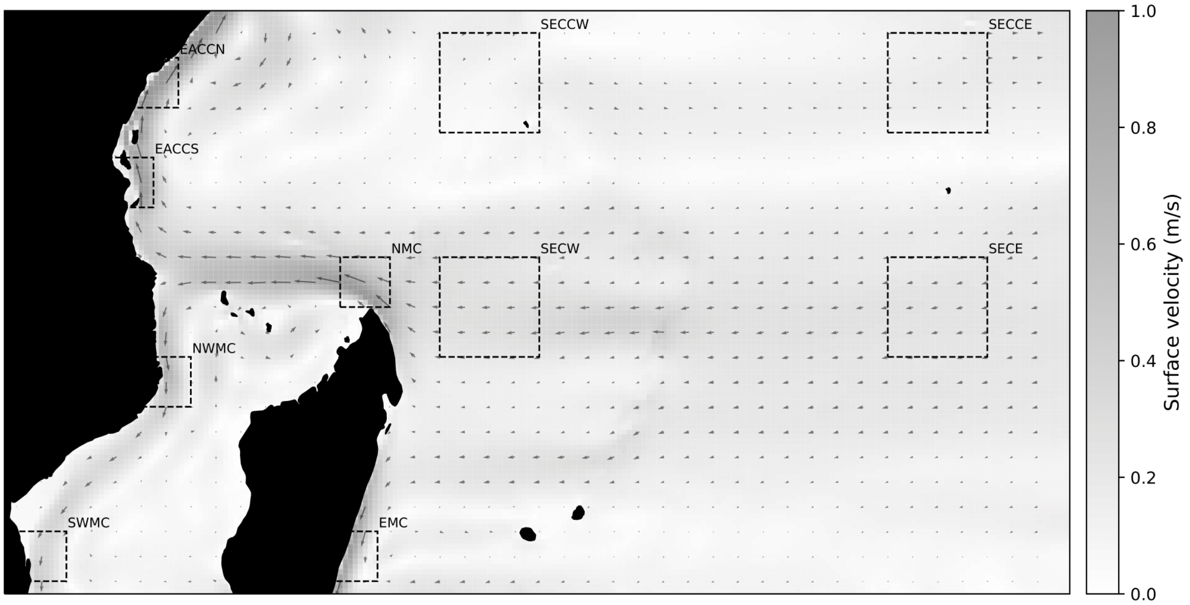

Figure S8: *Figures 7 and S9 show monthly mean surface currents averaged across the regions shown in this figure. The region codes are as follows.* ***SECW:*** *South Equatorial Current West;* ***SECE:*** *South Equatorial Current East;* ***NMC:*** *North Madagascar Current;* ***EMC:*** *East Madagascar Current;* ***NWMC:*** *Northwestern Mozambique Channel;* ***SWMC:*** *Southwestern Mozambique Channel;* ***EACCN:*** *East Africa Coastal Current North;* ***EACCS:*** *East Africa Coastal Current South;* ***SECCW:*** *South Equatorial Countercurrent West;* ***SECCE:*** *South Equatorial Countercurrent East.*

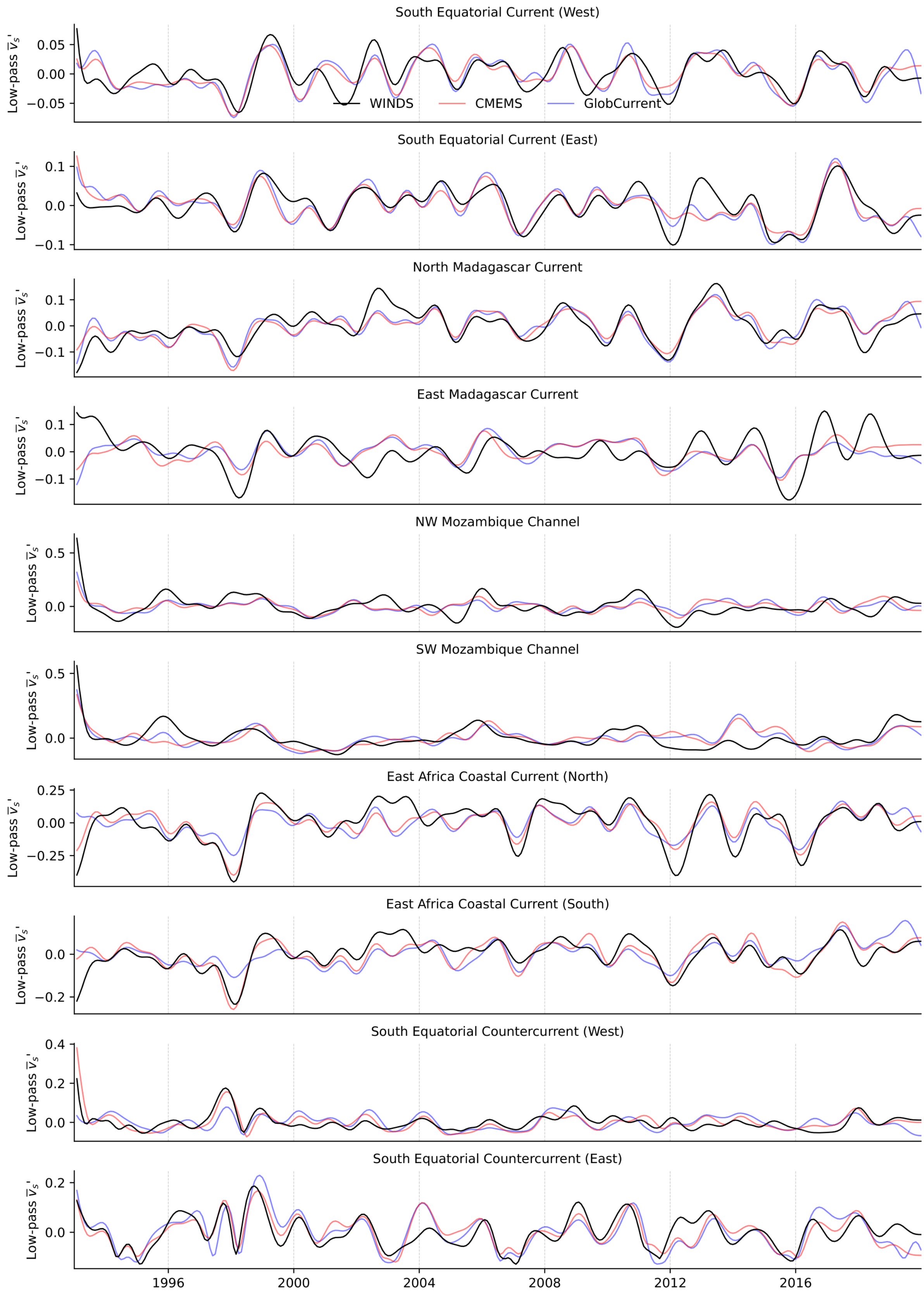

Figure S9: Low-pass filtered version of Figure 7, using a frequency cutoff of 1/480 days to remove intra-annual variability, and with the time-mean subtracted. As in Figure 7, WINDS is shown in black, CMEMS GLORYS12V1 in red, and Copernicus GlobCurrent in blue.

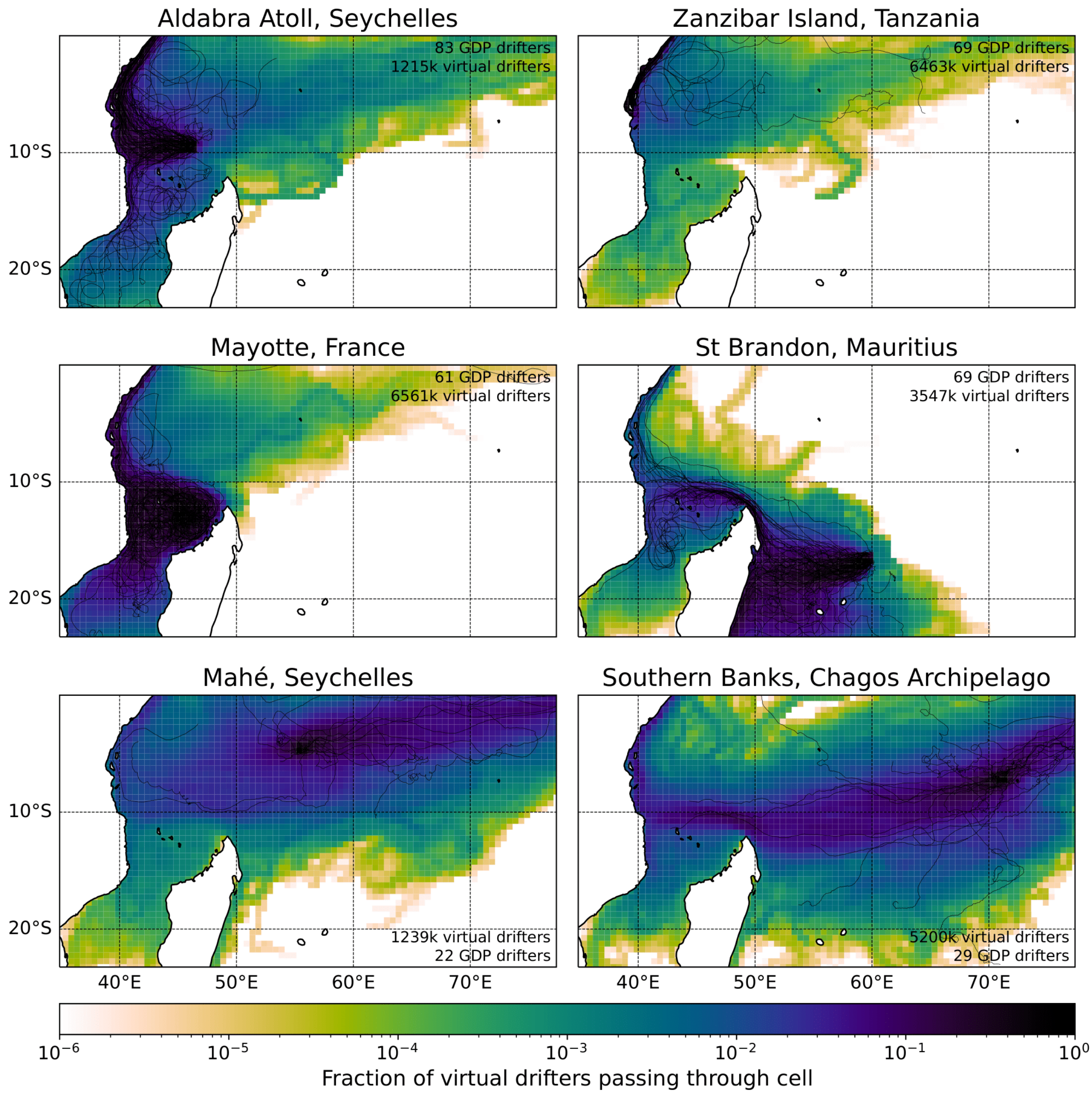

Figure S10: *Equivalent to Figure 8 in the main text, but with the colourbar extended to span low-probability dispersal events simulated by WINDS.*

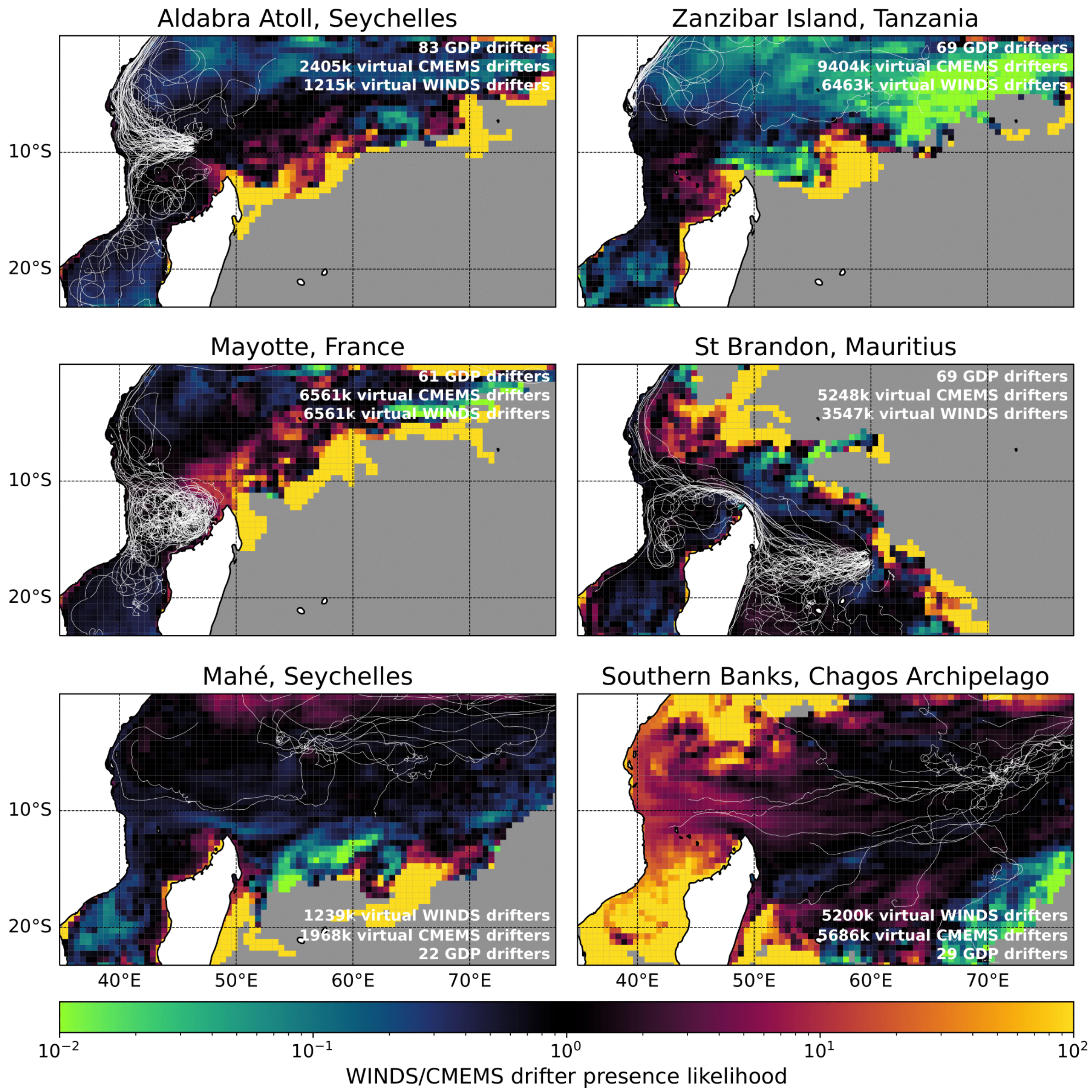

Figure S11: Relative difference in virtual drifter presence likelihood (within 120 days) between WINDS-M (as in Figure 8 in the main text) and the CMEMS GLORYS12V1 1/12º global ocean reanalysis. Cells where only WINDS and only GLORYS12V1 predicted dispersal to are saturated in yellow and green respectively. Cells where neither product simulated dispersal to are coloured in grey. Note that agreement is generally very high between the two, and (with reference to Figure 8 in the main text) significant relative disagreements only occur in regions predicted as low-probability by both ocean models. The only significant exceptions are greater connectivity between the East Africa Coastal Current and the South Equatorial Countercurrent predicted by GLORYS12V1, and greater westward flow in the South Equatorial Current from the Chagos Archipelago predicted by WINDS (both of which are supported by GDP drifters).

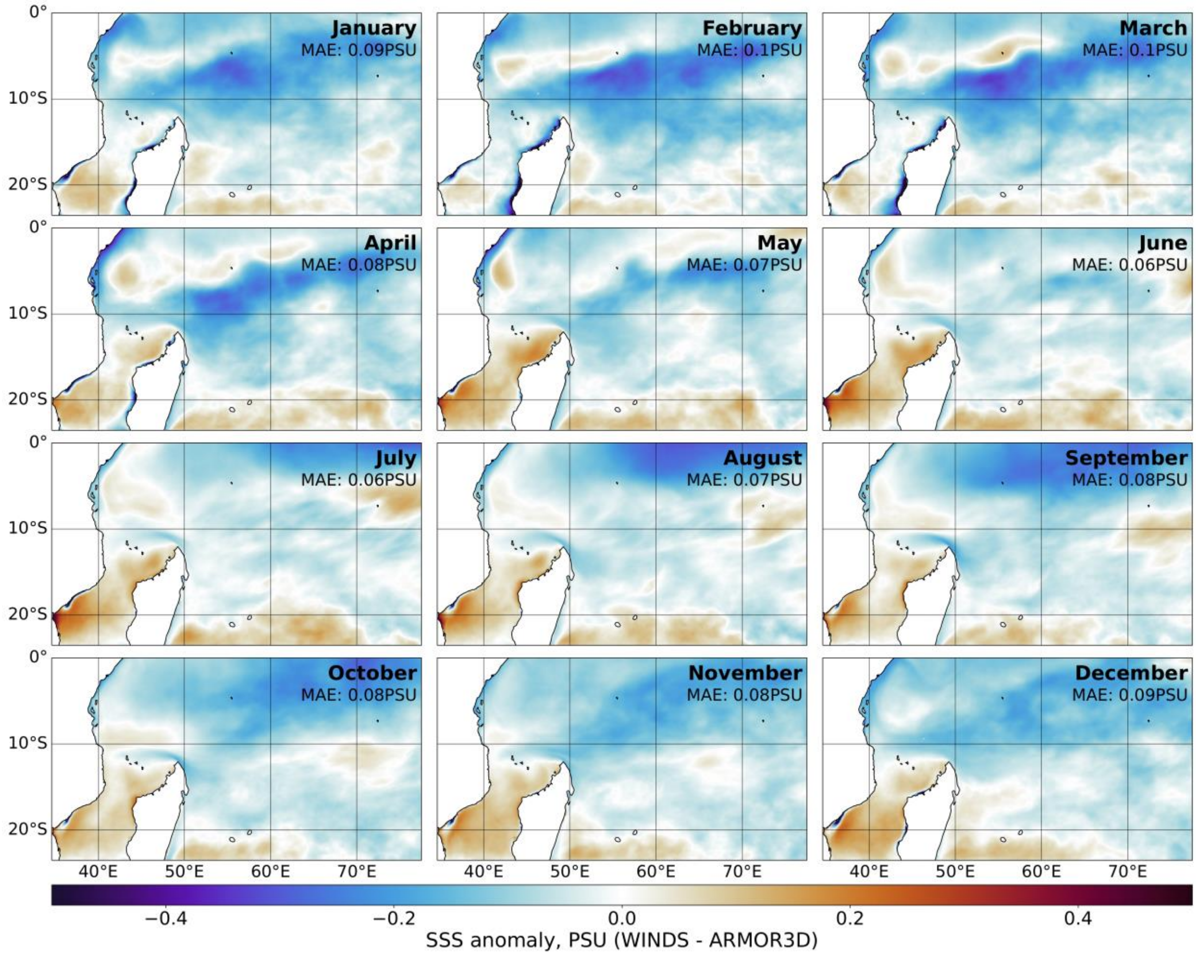

Figure S12: Difference between monthly climatological SSS simulated by WINDS, and in-situ derived SSS estimates from ARMOR3D. Blues indicate that WINDS simulates lower salinity (fresher), reds indicate that WINDS simulates higher salinity (saltier).

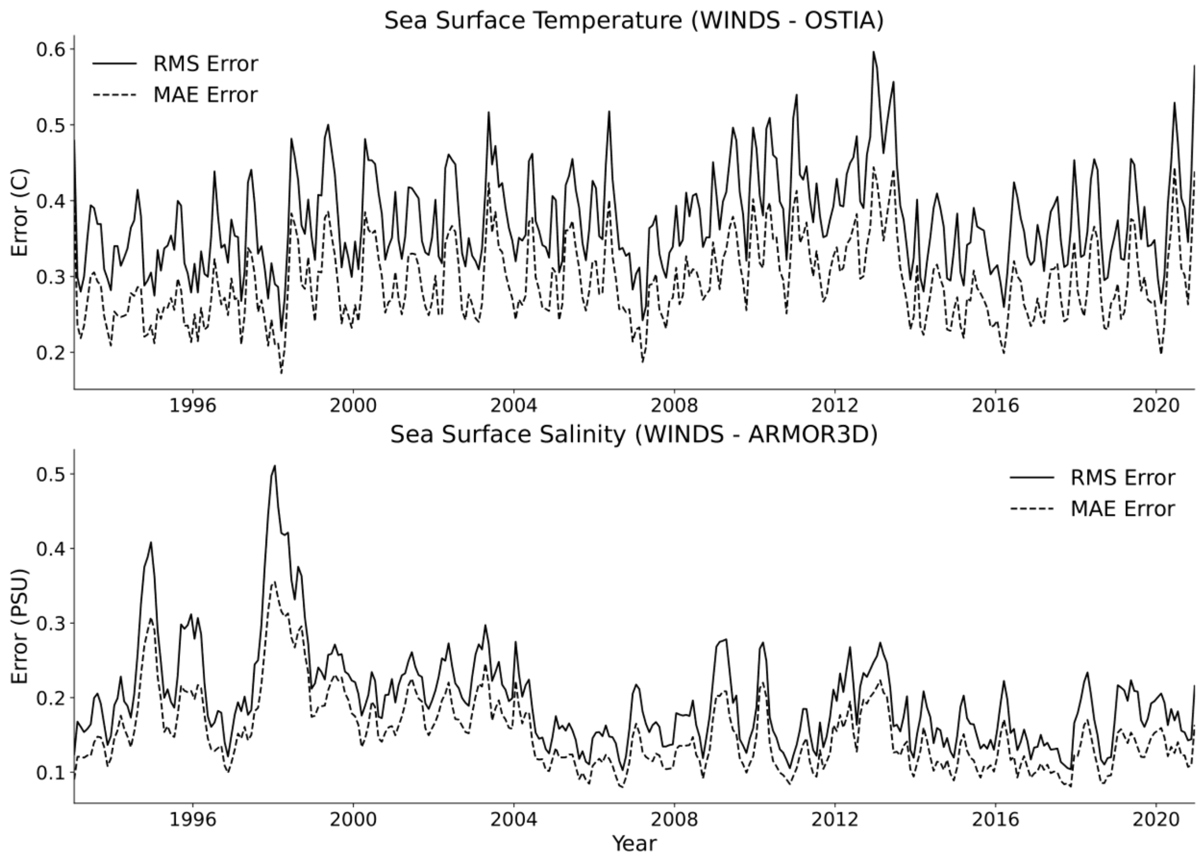

***Figure S13**: (Top) Root mean square (RMS) and mean absolute error (MAE) between monthly averages of WINDS and OSTIA SST from 1993-2020. (Bottom) RMS and MAE between monthly averages of WINDS and ARMOR3D SSS from 1993-2020.*

References

Egbert, G. D., & Erofeeva, S. Y. (2002). Efficient inverse modeling of barotropic ocean tides. *Journal of Atmospheric and Oceanic Technology*, *19*(2), 183–204. https://doi.org/10.1175/1520-0426(2002)019<0183:EIMOBO>2.0.CO;2